Low energy electron energy-loss spectroscopy of CF_3X (X=Cl,Br)

M. Hoshino and K. Sunohara
Department of Physics, Sophia University, Tokyo 102-8554, Japan

C. Makochekanwa
Department of Physics, Sophia University, Tokyo 102-8554, Japan and Department of Chemistry, Graduate School of Kyushu University, Fukuoka 812-8581, Japan

L. Pichl
Division of Natural Sciences, International Christian University, Tokyo 181-8585, Japan

H. Cho
Physics Department, Chungnam National University, Daejeon 305-764, Korea

H. Tanaka
Department of Physics, Sophia University, Tokyo 102-8554, Japan

(Received 13 November 2006; accepted 28 November 2006; published online 9 January 2007)

We report threshold electron energy-loss spectra for the fluorohalomethanes CF_3X (X=Cl,Br). Measurements were made at incident electron energies of 30 and 100 eV in energy-loss range of 4–14 eV, and at scattering angles of 4° and 15°. Several new electronic transitions are observed which are ascribable to excitation of low-lying states as well as are intrinsically overlapped in the molecules themselves. Assignments of these electronic transitions are suggested. These assignments are based on present spectroscopic and cross-section measurements, high-energy scattering spectra, and *ab initio* molecular orbital calculations. The calculated potential curves along the C–X bond show repulsive nature, suggesting that these transitions may lead to dissociation of the C–X bond. The present results are also compared with the previous ones for CF_3H, CF_4, and CF_3I. © *2007 American Institute of Physics*. [DOI: 10.1063/1.2424704]

I. INTRODUCTION

Freon and related halogen-substituted methane molecules CF_3X (X=H,F,Cl,Br,I) are, in general, important industrial molecules with wide-ranging applications such as semiconductor etching, refrigerants, fire extinguishers, etc. These tetrahedronlike systems are of fundamental interest for studying halogen substitutional effects as well. However, it has been widely recognized that CF_3Cl and CF_3Br are responsible, via photochemical mechanisms, for the depletion of the earth's ozone layer that protects our planet from the damaging effects of short wavelength solar radiation. Also CF_3H and CF_4 are strong greenhouse gases, and, therefore, must be replaced by the alternative compounds that have low global warming potentials. One possible replacement is CF_3I due to its weak C–I bonding. Thus, there are practical as well as fundamental interests in obtaining adequate spectroscopic information of the underlying electronic transitions for these fluorohalomethanes. Though these molecules have been investigated by a variety of techniques, the systematic study is less extensive in low-energy electron spectroscopy (EELS). The present work is concentrated with the electron impact excitation of the threshold electronic states of CF_3Cl and CF_3Br.

In low-energy electron impact spectroscopy, molecular transitions resulting from the transfer of energy from incident electrons to target molecules are not restricted by the optical selection rules. The low-momentum-transfer (high impact energy, low scattering angle) energy-loss spectrum is equivalent to the photoabsorption spectrum. The large-momentum-transfer (low impact energy, high scattering angle) spectra can reveal the presence of optically forbidden excitation. Thus, electron impact spectroscopy is a useful complement to conventional optical spectroscopy in the assignment of molecular electronic states.

In these regards, we will first briefly review the previous works in vacuum ultraviolet (VUV) and electron-impact spectroscopy on primarily CF_3Cl and CF_3Br. Photoabsorption spectra have been studied extensively by Doucet *et al.*[1] for both CF_3Cl and CF_3Br in the energy range from 6.2 to 10.33 eV. Gilbert *et al.*[2] and Doucet *et al.*[3] obtained the VUV spectra for CF_3Cl and CF_3Br, respectively, in the region extended to 19 eV. Photoelectron spectroscopy using resonance lamps was also carried by Doucet *et al.*[1] for CF_3Br above about 11 eV, and synchrotron radiation measurements by Bozek *et al.*[4] for CF_3X (X=F,Cl,Br,I). Biehl *et al.*[5] reported VUV and visible spectroscopy of CF_3X (X=H,F,Cl,Br) using fluorescence excitation and dispersed emission technique. Mason *et al.*[6,7] extensively studied photoabsorption of CF_3X (X=Cl,Br,I) using ASTRID synchrotron source and compared with the results from electron spectroscopy.

In the electron-impact studies, zero-angle electron energy loss spectroscopy for CF_3Cl was performed by King and McConkey[8] at the impact energy of 500 eV and by Zhang *et al.*[9] at the impact energy of 8 keV. Momentum-

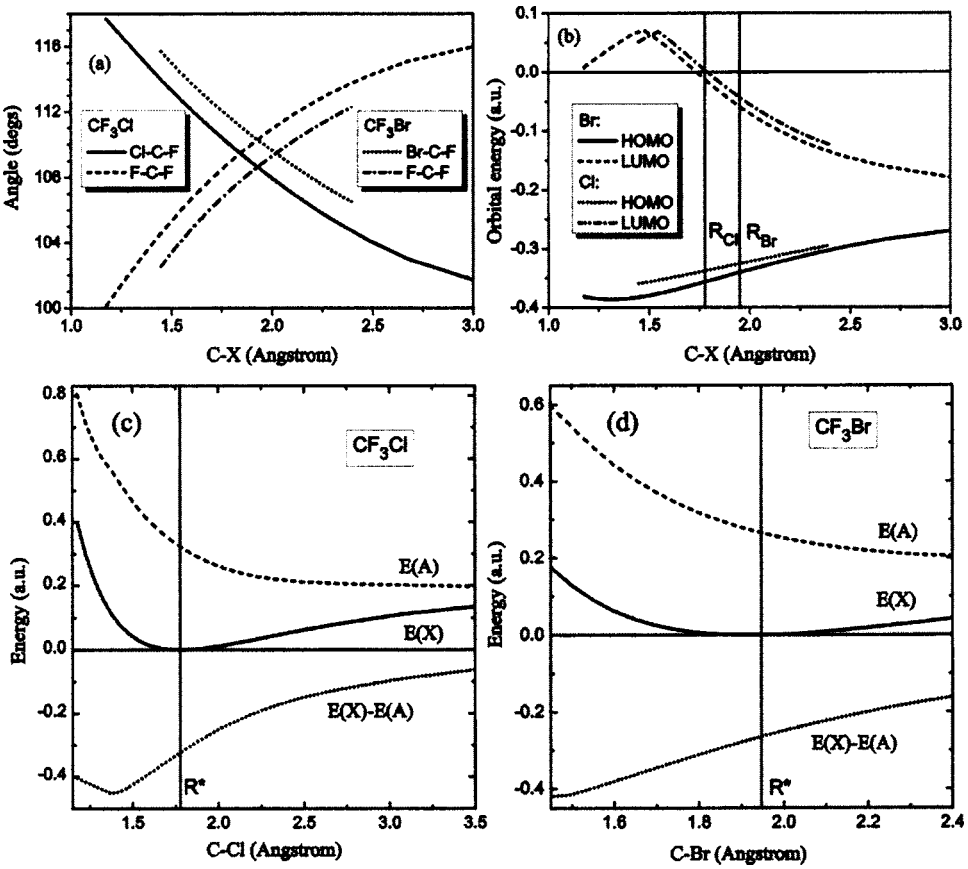

FIG. 1. *Ab initio* calculation of the CF_3X (X=Cl,Br) molecules: (a) bond angles and (b) HOMO and LUMO orbitals. The ground- and excited-state energies are shown in (c) for CF_3Cl (d) for CF_3Br, respectively.

transfer-resolved electron energy loss spectrum has given information on an unusually low-lying nondipole transition at 7.7 eV in CF_3Cl by Ying *et al.*[10] In addition, their *ab initio* generalized oscillator strengths (GOS) and single-excitation configuration interaction calculations showed that this transition is consistent with an electronic excitation from the nonbonding lone-pair orbital on the Cl atom [highest occupied molecular orbital (HOMO)] to the antibonding σ^* orbital [lowest unoccupied molecular orbital (LUMO)] leading to dissociation of the C–Cl bond. Chen *et al.*[11] studied the HOMO of CF_3Cl by binary $(e,2e)$ electron momentum spectroscopy. They calculated the position density and the result shows that the electron concentrates near the nucleus of the Cl atom implicating that this orbital is the chlorine's lone-pair orbital. And the momentum density shows that the orbital is p type. Sunohara *et al.*[12] measured absolute differential cross sections for elastic and vibrationally inelastic scattering of electrons from CF_3Cl and CF_3Br using a crossed-beam experiment in the energy range of 1.5–100 eV.

In this report, we have examined systematically the energy-loss region from 3 to 18 eV for all the halofluoromethanes up to CF_4 at incident electron energies of 30 and 100 eV and at the scattering angles of 4° (or 3° for CF_3H and CF_3I) and 15°. The molecular orbital calculations have also elucidated the threshold nature of low-lying electronic states in this halofluoromethane series.

II. EXPERIMENT

The electron spectrometer used in the present work has been described in detail elsewhere[13] and will be outlined only briefly here. The spectrometer consists of an electron gun with hemispherical monochromator, a molecular beam, and a rotatable detector (θ: 10° to 130°) with a second hemispherical system. A beam of molecules is crossed with a monoenergetic beam of electrons of fixed incident energy. At a particular scattering angle, electrons are detected having lost energies in the range from 3 to 18 eV. These energy-loss spectra are measured at the angles of 4° (or 3° for CF_3H and CF_3I) and 15° and for incident electron energies of 30 and 100 eV. For comparison purpose, an "optical absorption" type spectrum was taken using high-energy, low-angle conditions. A number of tube lenses in the spectrometer have been used for imaging and energy control of the electron beam, whose characteristics were carefully modeled by electron trajectory calculations. Both the monochromator and analyzer are enclosed in differentially pumped boxes to deduce the effect of background gases and to minimize any stray electron background. Overall resolution in all spectra was 25–35 meV (full width at half maximum). The angular scale was calibrated to ±1.5° by noting the symmetry of elastic scattering about the true zero-degree point. The energy scale was calibrated to the He 19.367 eV resonance at 90°.

III. THEORY

The adiabatic potential energy curves for the CF_3Cl and CF_3Br molecules in their electronic $X\ ^1A_1$ ground state were obtained at the density functional theory level. The three-parameter density functional of Becke was applied with the Lee, Young, and Parr correlation functions (Becke3LYP)

(GAUSSIAN 98).[14] Correlation consistent CC-pVTZ basis set, which accurately represents polarization effects along the carbon-halogen bonds, was used for the C, F, and Cl atoms. The core of the heavier Br atom was described by means of a pseudopotential, while a $[16s12p2d1f]$ Gaussian basis set contracted to $[3s3p2d1f]$ was employed for the seven valence electrons of bromine, hence reducing the number of active electrons in the CF_3Br calculation to 40 (in case of CF_3Cl all 50 electrons were active). In the equilibrium geometry, the CX distance is confirmed to be 1.78 and 1.95 Å for X=Cl and X=Br, respectively. The CF separation at the two different equilibrium geometries is very similar, however, 1.33 Å for X=Cl and Br, and maintains an almost constant difference of 0.015 Å for $|CX|$ ranging between 1.5 and 2.5 Å. The behavior of the optimized bond angles X–C–F and F–C–F along the CX stretch coordinate is shown in Fig. 1(a), which demonstrates the shape elongation of the molecule when X changes from Cl to Br. Eigenenergies of the HOMO ($6e$) and LUMO ($8a_1$) orbitals are plotted in Fig. 1(b). It is interesting to note the presence of the peak in the LUMO orbital energy for shorter $|CX|$ distances, where the dipole moment of the molecule diminishes (the carbon atom is symmetrically shielded by the electronegative halogens). The sign of the LUMO eigenvalue becomes negative with the increase of $|CX|$ distance, still quite before the equilibrium geometry is reached, which reflects the polar character of the actual CX bond (the dipole moments along the C_{3v} symmetry axis are about 0.43 D for X=Cl and 0.64 D for X=Br).

Figures 1(c) and 1(d) show the adiabatic potential energy curves and the first excited state for CF_3Cl and CF_3Br, respectively. The ground-state potential energy well is substantially broader in case of CF_3Br. The energies of the first excited state A in Figs. 1(c) and 1(d) were computed by the GAUSSIAN 03 single-excitation configuration interaction method. The potential energy curves correspond well to the HOMO-LUMO excitations [cf. the difference of $E(X)$-$E(A)$ in Fig. 1]. We note that the first excited state is strongly repulsive along the dipole axis of the molecule, which suggests that the electron-impact excitation of either molecule could result in the formation of X– along with a simultaneous fragmentation of the CF_3X molecule.

IV. RESULTS AND DISCUSSION

The energy-loss spectra of CF_3Cl and CF_3Br are presented together with other family of the fluoromethyl halides, i.e., CF_3H, CF_3I, and CF_4 in Fig. 2, in order to stress the commonality of their transitions. Rydberg transitions are presented using term values from the quantum defect interpretation with the photoelectron spectroscopy data available. Moreover, to compare with the spectra at two different impact energies of 30 and 100 eV, the data were normalized to each other at the strongest peak in each spectrum. Therefore, no direct comparison of the intensities between two impact energies can be made.

The electron configurations of the ground electronic state ($X\,^1A_1$) of the fluoromethyl halides CF_3X (X=H,Cl,Br,I), which has a tetrahedronlike geometry of C_{3v}, are as follows:

$(3a_1)^2(2e)^4(4a1)^2(5a_1)^2(3e)^4(4e)^4(5e)^4(1a_2)^2(6a_1)^2$ for CF_3H,

$(3a_1)^2(2e)^4(4a_1)^2(5a_1)^2(3e)^4(6a_1)^2(4e)^4(5e)^4(1a_2)^2(7a_1)^2(6e)^4$ for CF_3Cl,

$(3a_1)^2(2e)^4(4a_1)^2(5a_1)^2(3e)^4(6a_1)^2(4e)^4(5e)^4(1a_2)^2(7a_1)^2(6e)^4$ for CF_3Br,

and

$(4a_1)^2(5a_1)^2(3e)^4(6a_1)^2(4e)^4(5e)^4(1a_2)^2(7a_1)^2(6e)^4$ for CF_3I.

Also, under T_d symmetry of CF_4, the following configuration is obtained for the ground state:

$(1a_1)^2(1t_2)^6(2a_1)^2(3a_1)^2(2t_2)^6(4a_1)^2(3t_2)^6(1e)^4(4t_2)^6(1t_1)^6$ for CF_4

All excitations from these shells appear to follow a Rydberg pattern and have been classified. These molecules have been of great interests since they enable us to follow the changes that occur in the electronic structure and transitions of fluoromethane and the halogen lone pairs as a function of substitution and to gain knowledge on their excited states.

Overviews in Fig. 2 show the systematic trend that the thresholds for the electronic excitation and the ionization are shifting to lower energies as replacing with heavier halogen atoms in the same molecular symmetry C_{3v}. CF_4 is somehow exceptional in this comparison due to the molecular symmetry of T_d. Also, the l-s coupling interaction is dominating and then is observed clearly in the splitting of sharp structures for CF_3I. The electronic excitation in these molecular systems, moreover, may be divided into two contributions, one from the CF_3 component and the other from the substitution with a halogen atom. Of course, this substitution changes the actual molecular orbital. Therefore, molecular orbital calculation is needed to identify more precisely the observed spectra on the quantum chemical scheme. From a point of the molecular dissociation process, as mentioned above, the low lying triplet state is essential to produce the CF_3 radical,

besides the energies required for the dissociation are getting lower along the substitution as observed in Fig. 2. Those low-lying states are, for the first time, systematically identified as shown in Fig. 2 for CF_3Cl, CF_3Br, and CF_3I by the low energy electron impact spectroscopy at 30 eV.

The observations are summarized for each fluoromethyl halide as follows.

A. CF_3H

Following the previous measurements for the higher impact energies of 400 eV as well as for the photoelectron spectroscopy, the peaks at 10.92 and 11.95 are assigned to $6a_1 \rightarrow 3s$ and $6a_1 \rightarrow 3p$, and also the higher features at 12.58, 13.65, and 14.99 eV to $5e \rightarrow 3s$, $5e \rightarrow 3p$, or $4e \rightarrow 3s$ and $4e \rightarrow 3p$ transitions using term values, respectively. To compare CF_3H with CF_4, we recall the fluoromethane series CH_3F, CH_2F_2, CHF_3, and CF_4 including CH_4 (Refs. 15 and 16) and discuss the substitution effect of F atom from the CH_4 molecule. The highest orbital in CH_4 has the $1t_2$ symmetry of a carbon-hydrogen sigma bonding correlated only with the carbon $2p$ orbitals.[17] Along the halogen substitution from CH_4 to CHF_3, however, the uppermost component of the orbital $1t_2$ changes to more or less carbon-fluorine pi-antibonding character. This trend is just that presented by the first band at 10.92 eV in CF_3H, but which was observed at lower energy side around the same energies of ~9.42 eV in CH_4, CH_3F_2, and CH_2F_2. Thus, in CF_3H, the first two bands are assignable as $6a_1 \rightarrow 3s$ and $3p$.

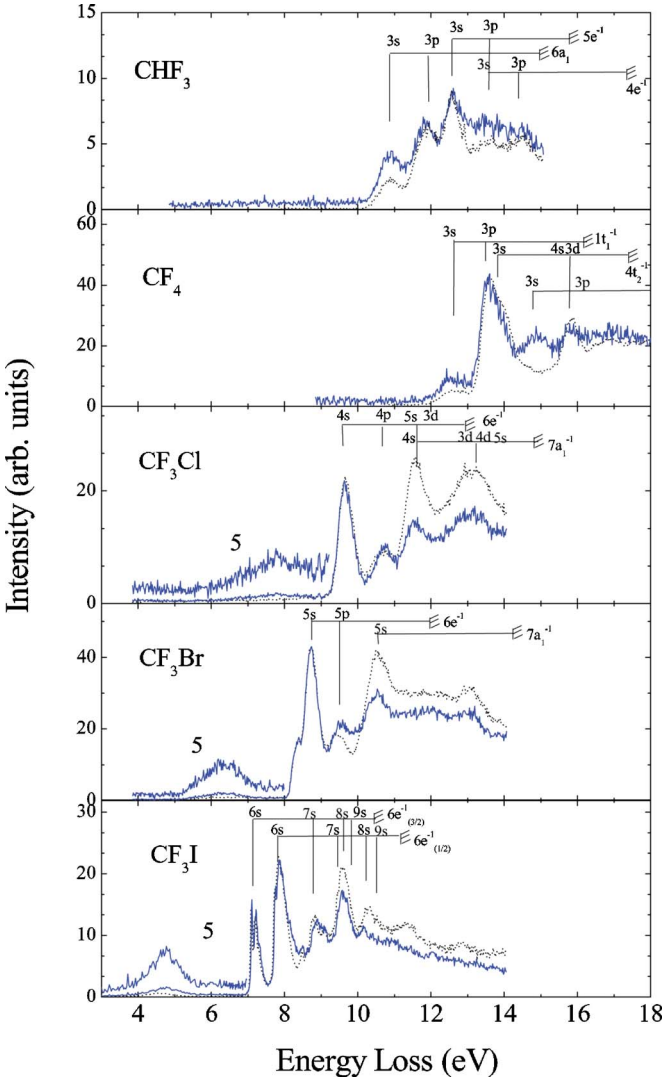

FIG. 2. (Color online) Electron energy loss spectra of CF_3X (X =H,F,Cl,Br,I) in the energy-loss regin from 3 to 18 eV at incident electron energies of 30 and 100 eV and at scattering angles of 4° (3° for CF_3H and CF_3I) and 15°, respectively. Solid line represents the data at lower energy/larger angle and dotted line higher energy/smaller angle.

B. CF_4

The EELS and photoelectron results show that all excitations from the ground state have been classified as Rydberg feature as shown in Fig. 2. The transitions of $1t_1 \rightarrow 3s$ and $1t_1 \rightarrow 3p$ or $5a_1$ correspond to the peaks at 12.6 and 13.7 eV, respectively. The two highest molecular orbitals, $1t_2$ and $4t_2$, are overlapped closely by 1.2 eV.[15] The former transition is expected to have a symmetry forbidden character due to weak oscillator strength of 0.024 ± 0.003. It is noted that the $1t_1$ orbital is composed of fluorine lone-pair pi orbitals, while $4t_2$ is carbon-fluorine sigma bonding. And, the latter transition indicates more or less carbon-fluorine pi-antibonding character due to HOMO→LUMO transition. The next higher features at 13.9 and 15.8 eV are assigned as the transitions of $4t_2 \rightarrow 3s$ and $4t_2 \rightarrow 4s$, $3d$ or $1e \rightarrow 3p$, respectively. The band at 14.8 eV is assignable as $1e \rightarrow 3s$, indicating a forbidden transition because this band is clearly observed in more favorable experimental condition at 30 eV for 20° than at 100 eV for 4°.

C. CF_3Cl

Figure 3 shows the electron energy loss spectra for CF_3Cl at the impact energy of 30 eV and the scattering angle

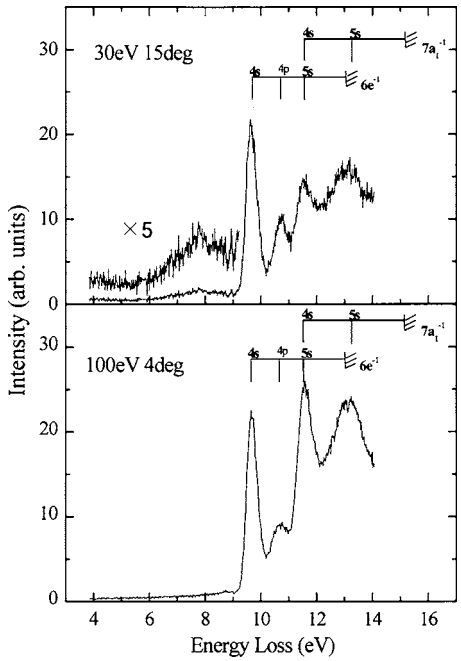

FIG. 3. Electron energy loss spectra of CF_3Cl in the energy-loss region from 4 to 14 eV at incident electron energies of 30 and 100 eV and at scattering angles of 15° and 4°, respectively.

of 15° and at the impact energy of 100 eV and the scattering angle of 4°. Based on numerous results from the photoelectron and the dipole EELS measurements, in the valence-shell electronic structures of CF_3Cl, the peaks at 9.6, 10.6, and 11.5 eV are assigned to $6e \rightarrow 4s$, $6e \rightarrow 4p$, $6e \rightarrow 5s$, $3d$, respectively, and peaks 11.5 and 13.2 eV are also identified as $7a_1 \rightarrow 4s$, $7a_1 \rightarrow 3d$, $4d$, $5s$, respectively, terminating to the Rydberg limit of $7a_1^{-1}$. $6e$ (HOMO) orbital is comprised essentially of a lone pair on Cl atom, and $7a_1$ is an orbital associated with C–Cl bonding. Therefore, the first ionization potential near 13.0 eV corresponds to taking out of one electron from the chlorine lone pair orbital, and the second ionization potential near 15.2 eV is related to the orbital populated in the C–Cl bond.[2] As shown in Fig. 3, around 7.7 eV, the peak with a low-lying nondipole character is clearly emerged at the impact energy of 30 eV for the scattering angle of 15° but not at the impact energy of 100 eV for 5°. This nondipole electronic transition with a quadrupole characteristic is observed for the first time in the electron energy loss experiments. However, it was previously observed by the different experimental method using the momentum-transfer-resolved electron loss spectroscopy[10] at 2.5 keV, which was assigned as $6e(\text{HOMO}) \rightarrow 8a_1(\text{LUMO})$ transition related an electronic transition from a nonbonding Cl $3p$ orbital (HOMO) to an antibonding $\sigma^*_{\text{C–Cl}}$ orbital (LUMO). In the case of $n_{\text{Cl}3p} \rightarrow \sigma^*_{\text{C–Cl}}$ transition, the overlap between the initial-state and final-state orbital wave functions occurs mostly at Cl site. The transition moment of this electronic transition is expected to resemble that of p-to-p transition in Cl atom which explains the quadrupole nature.[10,18–20] In the study by Ying *et al.*,[10] the GOS of this transition has been determined and found to have a shape characteristic of a quadrupole transition with a maximum at around 1 a.u. of the momentum transfer. While similar low-lying quadrupole transitions have been observed for other members of CFC, no such nondipole transition is found in the case of CF_4, suggesting the involvement of Cl atoms in this quadrupole feature. The LUMO was found to be a repulsive potential character by McLean and Chandler.[21]

D. CF_3Br

The electron energy loss spectrum for CF_3Br is given in Fig. 4. As assigned previously from the UV spectrum data, the strong bands at 8.7 and 9.53 eV are associated with the Br $6e^{-1}$ ionization at 12.0 eV, the transitions from the bromine lone pair orbital to $5s$ and $5p$ terminating orbitals, respectively. The former one has a shoulder at 8.42 eV, which is due to spin-orbit splitting and there is no corresponding shoulder observed for CF_3Cl, while this splitting is much clearer for CF_3I than for CF_3Br. The peak at 8.7 eV is a singlet-singlet transition and the shoulder at 8.42 eV has a singlet-triplet character.[1] However, Eden *et al.*[7] argue that the relative intensity of the two peaks at 8.42 and 8.7 eV are approximately equal in 100 eV, 4° and 30 eV, 15° spectra (see Fig. 2) and this lack of angular dependence strongly suggests that both features are due to singlet to singlet transitions. This leads Eden *et al.* to suggest that the broad feature peaked at 8.42 eV is due to the promotion of an electron

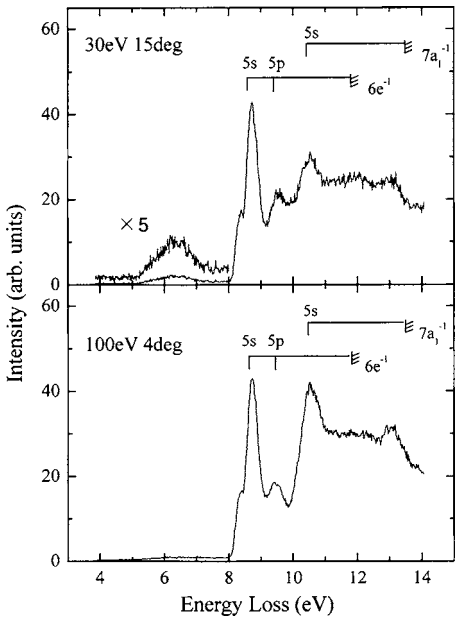

FIG. 4. Electron energy loss spectra of CF_3Br in the energy-loss region from 4 to 14 eV at incident electron energies of 30 and 100 eV and at scattering angles of 15° and 4°, respectively.

from the second highest occupied molecular orbital (MO) (C–Br σ) to the LUMO (C–Br σ^*). The band at 10.54 eV corresponds to the transition of $7a_1 \rightarrow 5s$. The first ionization potential corresponds to Br lone pair orbital, and the second ionization potential belongs to bonding orbitals of mainly C–Br character. Compared to CF_3Cl, the ionization potentials of $6e$ and $7a_1$ for CF_3Br are lower by around 1 eV.[5] Though, as mentioned above, no direct comparison is possible in the intensity, the minimum and the peak positions are apparently changed in the spectral shapes around 9.53 eV due to the optical forbidden transitions involved strongly. The most prominent feature is a clear observation again for the low-lying electronic excitation states near threshold around 6.5 eV at electron impact energy only of 30 eV not of 100 eV. But, this feature is not mainly due to the optical forbidden character, like a triplet state, because the weak transition has been also observed in the vacuum ultraviolet spectrum.[1]

E. CF_3I

The assignments for the transitions are reported previously (Ref. 6 and references therein). Briefly, the weak broad band observed around 4.6 eV was identified as $5p\pi \rightarrow \sigma^*$ (C–I) transition which is composed in the $^3Q_1$ (4.10 eV), $^3Q_0$ (4.70 eV), and $^1Q_1$ (5.34 eV) states due to the spin-orbit coupling and exchange interactions as confirmed by the photoabsorption results. The $^3Q_0$ and $^1Q_1$ states are enhanced at 4.70 and at 5.34 eV for the impact energy of 30 and 100 eV, respectively, as shown in Fig. 2. Moreover, the resultant excited states, i.e., the broad features without a fine vibrational progression, are leading to dissociation along the C–I stretch coordinate due to occupation of the C–I ($^2P_{3/2}$, $^2P_{1/2}$) antibonding state, respectively, where $5p\pi$ is the outermost lone-pair π orbital of I atom and σ^* is antibonding carbon iodide sigma MO. The peaks at 7.13 and at 7.75 eV are assigned as

$6e_{3/2} \rightarrow 6s$ and $6e_{1/2} \rightarrow 6s$ Rydberg transitions, giving rise to four components: $^2E_{3/2}[2]$, $^2E_{3/2}[21]$, $^2E_{1/2}[0]$, and $^2E_{1/2}[1]$ again due to the spin-orbit and exchange interactions. On those bands with the bound state nature, the weak vibrational progressions are visible even with the present energy resolution of our spectrometer though the bands exhibit clearly structure dominated by the vibrational progressions in their high resolution photoabsorption spectra. The further bands being observed at 8.8 and 9.6 eV are tentatively attributed to the transition of $6e_{3/2} \rightarrow 7s$ and $6e_{1/2} \rightarrow 7s$, and weak features observed between 8.5 and 8.6 eV may be due to a vibrational progression and the band between 9.1 and 9.4 eV due to excitation of yet another state. There is no information available for a series of the bands above 10 eV, and thus a full electronic structure calculation deriving the energies of high-lying Rydberg series would be desired.

V. CONCLUSIONS

By varying the scattering angle and incident energy, we have studied systematically a low-lying transition in the valence shells of the halogen-substituted methane molecules CF_3X (X=H,F,Cl,Br,I). As mentioned above, those low-lying states are, for the first time, systematically identified for CF_3Cl, CF_3Br, and CF_3I by the low energy electron impact spectroscopy at 30 eV, in which the large-momentum-transfer (low impact energy, high scattering angle) spectra are, in general, favorable to detect the presence of optically forbidden excitations. Furthermore, including CF_4, these all four molecules have a lone-pair electron in each halogen atom, but not in the halogen atom of CF_3H. From the molecular-symmetry point of view, former three belong to C_{3v} but CF_4 belongs to a different and much higher symmetry of T_d. Therefore, it is concluded that the halogenated CF_3Cl, CF_3Br, and CF_3I with C_{3v} symmetry as well as a lone-pair electron reveal the low-lying weak band, leading to dissociation of the molecules into the CF_3 radical along the C–X molecular axis. Furthermore, the CIS molecular calculation reveals the repulsive potential nature of LUMO for these two molecules, which supports the present experimental results. The direct product table for the symmetry group C_{3v} indicates that the $1a_1 \rightarrow 1e$ transition is both dipole allowed and quadrupole allowed, and the small transition dipole moment therefore suggests that this transition can be attributed predominantly to quadruple interactions. In addition, as indicated by the dominant molecular orbital coefficients, the $1a_1 \rightarrow 1e$ transition corresponds to a transition from an essentially nonbonding Cl $3p$ orbital to an antibonding p-σ^* C–Cl orbital. The p-to-p transition is therefore consistent with a quadrupole transition. It should also be noted that a vertical transition originated from the ground vibrational level of the $^1A_1$ state terminates at the repulsive part of the potential energy curve of the ^1E state above its dissociation limit.

ACKNOWLEDGMENTS

This work was performed with the support and under the auspices of the CUP, the IAEA's Co-ordinated Research Program, MEXT, and JAEA. One of the authors (C.M.) had been also thankful to the Japan Society for Promotion of Science for financial support under Grant No. P04064. One of the authors (L.P.) also acknowledges partial support by the Academic Frontier Program of MEXT. One of the authors (H.C.) acknowledges the support from the Korea Research Foundation (2006-311-C00031).

[1] J. Doucet, P. Sauvageau, and C. Sandorfy, J. Chem. Phys. **58**, 3708 (1973).
[2] R. Gilbert, P. Sauvageau, and C. Sandorfy, J. Chem. Phys. **60**, 4820 (1974).
[3] J. Doucet, R. Gilbert, P. Sauvageau, and C. Sandorfy, J. Chem. Phys. **62**, 366 (1975).
[4] J. D. Bozek, G. M. Bancroft, J. N. Cutler, K. H. Tan, and B. W. Yates, Chem. Phys. **132**, 257 (1989).
[5] H. Biehl, K. J. Boyle, R. P. Tuckett, H. Baumgartel, and H. W. Jochims, Chem. Phys. **214**, 367 (1997).
[6] N. J. Mason, P. Limao-Vieira, S. Eden *et al.*, Int. J. Mass. Spectrom. **223–224**, 647 (2003).
[7] S. Eden, P. Limao-Vieira, S. V. Hoffman, and N. J. Mason, Chem. Phys. **323**, 313 (2006).
[8] G. C. King and J. W. McConkey, J. Phys. B **11**, 1861 (1978).
[9] W. Zhang, G. Cooper, T. Ibuki, and C. E. Brion, Chem. Phys. **151**, 343 (1991).
[10] J. F. Ying, C. P. Mathers, K. T. Leung, H. P. Pritchard, C. Winstead, and V. McKoy, Chem. Phys. Lett. **212**, 289 (1993).
[11] X. J. Chen, C. C. Jia, C. K. Xu, G. Ouyang, L. L. Peng, S. X. Tian, and K. Z. Xu, Chem. Phys. Lett. **319**, 76 (2000).
[12] K. Sunohara, M. Kitajima, H. Tanaka, M. Kimura, and H. Cho, J. Phys. B **36**, 1843 (2003).
[13] H. Tanaka, L. Boesten, D. Matsunaga, and T. Kudo, J. Phys. B **21**, 1255 (1988).
[14] M. J. Frisch G. W. Trucks, H. B. Schlegel*et al.* Computer code GAUSSIAN 98 (Gaussian, Pittsburgh, 1995); Basis sets are described by W. J. Hehre, L. Radom, P. v. R. Schleyer, and J. A. Pople, *Ab Initio Molecular Orbital Theory* (Wiley, New York, 1986); Density functional theory (Becke3LYP) is described by W. Kohn, A. D. Becke, and R. G. Parr, J. Phys. Chem. **100**, 12974 (1991).
[15] W. R. Harshbarger, M. B. Robin, and E. N. Lassettre, J. Electron Spectrosc. Relat. Phenom. **1**, 319 (1972).
[16] M. B. Robin, *Higher Excited States of Polyatomic Molecules* (Academic, New York, 1974), Vol. 1, p. 179.
[17] M. A. Dillon, R.-G. Wang, and D. J. Spence, J. Chem. Phys. **80**, 5581 (1984).
[18] J. F. Ying and K. T. Leung, J. Chem. Phys. **101**, 7311 (1994).
[19] J. F. Ying and K. T. Leung, J. Chem. Phys. **101**, 8333 (1994).
[20] K. T. Leung, J. Electron Spectrosc. Relat. Phenom. **100**, 237 (1999).
[21] D. McLean and G. S. Chandler, J. Chem. Phys. **72**, 5639 (1980).